13th International Conference on Fusion Reactor Materials (ICFRM-13)
10.-14. December 2007, Nice, France

Improvement of Thermal Shock Resistance of Isotropic Graphite by Ti-doping

I. López-Galilea[1*], N. Ordás[1], C. García-Rosales[1], S. Lindig[2]

[1]CEIT and Tecnun (University of Navarra), 20018 San Sebastian, Spain

[2] Max-Planck-Institut für Plasmaphysik, EURATOM Association, D-85748 Garching, Germany

Abstract

Ti-doped isotropic graphite is a promising candidate material for the strike point area of the ITER divertor due to its reduced chemical erosion by hydrogen bombardment and its high thermal shock resistance, mainly due the catalytic effect of TiC on the graphitization leading to an increase of thermal conductivity and to higher mechanical strength. Several manufacturing parameters such as oxidative stabilization treatment, carbonization cycle, graphitization temperature and dwell time during graphitization have been investigated in order to establish a relationship between these parameters and the final properties.

*Corresponding author
Inmaculada López-Galilea
CEIT and Tecnun (University of Navarra)
Pº de Manuel Lardizabal, 15
E-20018 San Sebastián, Spain.
Tel and Fax.:+(34) 943 21 28 00
E-mail address: ilopez@ceit.es

1. Introduction

Carbon fiber-reinforced carbon (CFC) is the present candidate material for the strike point area of the ITER divertor due to its ability to withstand excessive heat loads during edge-localized modes (ELMs) and plasma disruptions [1]. However, chemical erosion of carbon under hydrogen bombardment from the plasma involves serious disadvantages for this application [2] (replacement and serious safety concerns due to tritium co-deposition [1,3]). In addition, CFCs have an inherent anisotropy, resulting in preferential erosion during transient heat loads, and their manufacturing process is long and complex.

Doping of carbon with small amounts of certain elements is known to reduce chemical erosion [4,5] thanks to dopant enrichment at the surface due to preferential sputtering of carbon. Additionally, other required properties such as a high thermal shock resistance can also be improved by doping carbon with suitable elements taking advantage of their catalytic effect on the graphitization [6,7]. For an effective improvement of all properties, a very fine and homogeneous dopants' distribution is required.

In this work finely dispersed Ti-doped graphites have been manufactured using a synthetic mesophase pitch as raw material. The aim is to improve substantially the thermal conductivity and mechanical strength and thus, the thermal shock resistance of graphite, reducing at the same time the chemical erosion by hydrogen bombardment. In this way it is expected to obtain a material able to compete with present CFC candidate materials. The results of this material development are shown in this paper.

Thermal load experiments were performed in the electron beam test facility JUDITH-I at Forschungszentrum Jülich, and erosion measurements by deuterium bombardment were performed at the high current ion source of the Max-Planck-Institute for Plasmaphysics in Garching. The results of these tests are reported in [8].

2. Experimental

2.1 Materials manufacturing

A self-sintering synthetic naphthalene-derived mesophase pitch named *AR* has been used as starting carbon raw material. *AR* exhibits excellent graphitizability, high chemical purity and consistent quality. Due to its low viscosity at the softening point, it is necessary to modify the initial viscosity of *AR* by an oxidizing treatment (called oxidative stabilization) at moderate temperatures (<350ºC) in an oxygen-rich atmosphere previous to mixing and forming [4,9]. The average particle size (APS) of the stabilized powder is <10 μm.

As main dopant TiC (APS 130 nm) has been selected because it leads to a considerable reduction of chemical erosion by hydrogen bombardment [3,5], and it contributes to a significant increase in thermal conductivity and improvement of mechanical strength due to the catalytic effect of this carbide on the graphitization [6,7]. Some samples were additionally doped with α-SiC, (APS 20 nm) to obtain a further improvement of the thermal conductivity due to the high graphitization degree of the carbon precipitated by the decomposition of SiC [10].

The mixtures were molded by cold isostatic pressing (CIP) between 125 and 200 MPa. Carbonization was performed at 1000°C in N_2 atmosphere and graphitization was performed in He atmosphere at temperatures between 2400 and 2765°C. Holding at the maximum graphitization temperature ranged from 15 to 60 min. The samples containing SiC in addition to TiC were graphitized with a very slow heating rate in the temperature range around the decomposition temperature of SiC (2540°C [11]), to avoid swelling and cracking due to fast Si evaporation.

2.2 *Materials characterization*

For materials characterization, the following parameters were measured:

- The carbide distribution was analyzed by optical microscopy and scanning electron microscopy (SEM).
- The geometrical density, ρ_G, was determined from the dimensions and weight of the samples. The true density, ρ_T, and the open porosity, P_{OPEN}, were measured with a He pycnometer, and the total porosity, P_{TOT}, was calculated from the geometrical and true densities.
- The crystallite size perpendicular to the basal planes, L_c, (as an indicator of the graphitization degree) was measured by X-ray diffraction using the Cu-Kα_1 radiation.
- The flexural strength, σ_f, was determined by a three-point-bending test on four beams of each material.
- The thermal diffusivity of representative samples was measured by the laser flash method over the temperature range 20-1200ºC. The thermal conductivity, K(T), was determined from the thermal diffusivity, the bulk density and the heat capacity.

3. Results and discussion

In order to study the influence of the moulding pressure on the final properties, bars made of *AR* doped with TiC (this material is named henceforth *AT*) were moulded between 125 and 200 MPa and graphitizated at 2750ºC for 15 min. In Table 1, density, porosity and flexural strength are shown for all doped materials as well as for the undoped material, *A*, for comparison. The optimum pressure for obtaining the best values of ρ_G, P_{TOT} and σ_f is 175 MPa. Higher moulding pressures may lead to cracks by the exit of volatiles during the carbonization process.

A fine and homogeneous carbide distribution was obtained after carbonization, demonstrating that the mixing procedure was adequate. The carbide coarsening observed after graphitization, Fig. 1, evidences the high mobility of the carbides in the carbonaceous matrix [4,6]. The microstructure was not significantly affected by the different moulding pressures.

The L_c value is independent on the moulding pressure. After graphitization at 2750ºC, the L_c value increases considerably (> 40 nm) compare to the undoped material *A* (L_c 31 nm). This increment is due to the dissolution of unordered carbon in liquid nm-sized TiC particles followed by the precipitation as ordered graphite [4]. Fig. 2 shows that the thermal conductivity of *AT-175* is considerably improved compared to the one of *A*.

After optimizing the moulding pressure for the *AT* materials, a new batch of *AT-175* samples, named henceforth simply *AT*, was manufactured with the aim to improve the thermal conductivity, modifying exclusively the graphitization parameters. In addition, new materials were manufactured adding also a small amount of SiC, *ATS*, with the same main goal. Table 2 shows the evolution of properties with temperature for the *ATS* material and the new *AT* material.

ATS shows a change in the character of porosity (open/closed) only relevant at the highest temperature, due to the strong TiC movement through the carbonaceous matrix; besides, Si evaporation contributes to increase the total porosity at the highest temperature. Additionaly, the Si formed by the decomposition of SiC may react with disordered carbon, and the C precipitated by the decomposition of this carbide has a high graphitization degree [10], contributing to increase the thermal conductivity, as demonstrates the high thermal conductivity achieved (195 W/mK at room temperature) compared to *AT-175*, Fig. 2. After graphitization at 2400 and 2765ºC, an inevitable decrease in strength is observed due to the recrystallization process taking place. In comparison to *A* (Table 1), doping with Ti leads to a remarkable increase in σ_f thanks to the refoircement effect of TiC [4,8]. The increase of porosity resulting both from Si evaporation (for those samples containing SiC) and from slightly incorrect stabilization parameters of the AR raw material is detrimental for the mechanical properties.

After carbonization, *ATS-1000* shows a turbostratic structure with very low crystalline order (L_c values between 1 and 2 nm); the carbide distribution, Fig. 3a, is homogeneous and it is not possible to distinguish Si from Ti. Graphitization at 2400ºC, Figure 3b, results in slight carbide coarsening. Under this condition, all SiC remains in the bulk material. Finally, in *ATS-2765* strong carbide coarsening occurs, Figure 2c, with the formation of areas almost free of carbides. The final particle size of some SiC was similar in some cases to that of TiC, despite of their initial particle size, 20 and 130 nm, respectively. This change in both the size and shape of the carbides evidences the

extremely high mobility of the carbides in the carbonaceous matrix, which arises from local carbide fusion and subsequent movement of the melt during catalytic graphitization [4].

The special graphitization cycle performed for *AT* leads to the highest K(RT) value, 217 W/mK, and acceptable values are achieved for the rest of properties.

Fracture surfaces were analyzed by SEM to identify the defect responsible for fracture initiation. In those undoped samples in which this defect could be found, it corresponded mostly to large mesophase particles, fractured by cleavage, Fig. 4a. In the majority of the doped samples the fracture was initiated in graphitic structures thicker than those observed in the rest of the carbonaceous matrix, associated with local heterogeneities in the distribution of carbides, Fig. 4b. The periphery of the majority of the examined surfaces showed a carbide depletion of about 50 μm.

4. Conclusions

In this work Ti and Ti/Si-doped isotropic graphite have been developed using self-sintering synthetic mesophase pitch AR as starting material. Dopant addition and a rigorous control of the manufacturing parameters contribute to improve significantly the final properties, especially the thermal conductivity and the mechanical strength, achieving at the same time a good carbide distribution. These results together with the measurements of the total erosion yield by deuterium bombardment and of the thermal shock resistance during disruption-like electron beam loads performed on these materials [8] let assume that Ti-doped graphites can be promising armour materials for divertor plasma-facing components.

Acknowledgements

This work has been funded by the European Community within the ExtreMat Integrated Project of the FP6 (NMP3-CT-2004-500253), and by the Spanish Ministry for Science and Education (ENE2006-14577-C04-04/FTN and MAT2004-22921-E).

References

[1] G. Federici et al., Key ITER plasma edge and plasma–material interaction issues, J. Nucl. Mater. 313-316 (2003) 11-22.

[2] J. Roth, Status of knowledge of chemical erosion of carbon and critical issues for extrapolation to ITER, Phys. Scr. T124 (2006) 37-43.

[3] E. de Juan Pardo et al., Erosion Processes of Carbon Materials under Hydrogen Bombardment and their Mitigation by Doping, Phys. Scr. T111 (2004) 62-67.

[4] N. Ordás, C. García-Rosales, S. Lindig, M. Balden, H. Wang, Effect of catalytic graphitization on the thermo-mechanical properties of isotropic graphite doped with metallic carbides, Phys. Scr. T111 (2004) 190-194.

[5] M. Balden, C. Adelhelm, E. de Juan Pardo, J. Roth, Chemical erosion by deuterium impact on carbon films doped with nanometre-sized carbide crystallites, J. Nucl. Mater. 363 (2007) 1173-1178.

[6] C. García-Rosales, N. Ordás, E. Oyarzabal, J. Echeberria, M. Balden, S. Lindig, R. Behrisch, Improvement of the thermo-mechanical properties of fine grain graphite by doping with different carbides. J. Nucl. Mater. 307-311 (2002) 1282- 1288.

[7] I. López-Galilea, C. García-Rosales, G. Pintsuk and J. Linke, Development of finely dispersed Ti- and Zr-doped isotropic graphites for the divertor of next step fusion devices. Phys. Scr. T128 (2007) 60–65.

[8] C. García-Rosales, I. López-Galilea, N. Ordás, C Adelhelm, M. Balden, G. Pintsuk, M. Grattarola, C. Gualco. J. Nucl. Mater, these proceedings.

[9] F. Fanjul, M. Granda, R.Santamara, R. Menendez, Pyrolysis behaviour of stabilized self-sintering mesophase, Carbon 41 (2003) 413-422.

[10] Haipeng Qiu, Yongzhong Song, Lang Liu, Gengtai Zhai, Jingli Shi, Thermal conductivity and microstructure of Ti-doped graphite. Carbon 41 (2003) 973–978.

[11] O. Kubaschewski, E.L.L. Evans, C.B. Alcock, Metallurgical Thermochemistry, 4th, Pergamon Press, Oxford, 1967.

Table Captions

Table 1: Typical properties of the undoped (*A*) and 4 at.% Ti-doped materials (*AT*) at different CIP.

Table 2: Properties of Ti/Si-doped (*ATS*) and Ti-doped (*AT*) materials for different conditions.

Figure Captions

Figure 1: Carbide coarsening after graphitization of *AT* graphite.

Figure 2: Thermal conductivity *vs*. temperature for representative samples of undoped, Ti-doped and Ti/Si-doped materials

Figure 3: Carbide distribution in *ATS* materials: a) after carbonization at 1000ºC; b) after graphitization at 2400ºC; c) after graphitization at 2765ºC.

Figure 4: Fracture surfaces after bending test: a) fracture by cleavage in undoped graphite; b) fracture initiation in carbide heterogeneities present in doped graphite.

Table 1

Sample code	CIP (MPa)	Graphitization (ºC, min)	ρ_G (g/cm^3)	P_{TOT} (Vol %)	P_{OPEN} (Vol %)	Lc (nm)	σ_f, (MPa)
A	175	2765, 30	1,86 -1,94	13 - 17	~90% P_{TOT}	31± 3	50 ± 10
AT-125	125	2750, 15	2.123	8.96	5.6		113
AT-150	150		2.145	8.01	3.6	42	116
AT-175	175		2.159	7.41	0	40	108
AT-200	200		2.164	7.19	0	41	95

Table 2

Sample code	Dopant	Conditions (ºC, min)	ρ_G (g/cm^3)	P_{TOT} (Vol %)	P_{OPEN} (Vol %)	Lc (nm)	σ_f (MPa)	K(RT) (W/mK)
ATS-green	4 at.%Ti + 0.5 at%Si	green	1.44 ± 0.0	12.2 ± 0.3	P_{TOT}	-	-	-
ATS-1000		1000, 60	1.87 ± 0.1	16.4 ± 1.2	12.9 ± 0.2	~ 1.7	146 ± 10	-
ATS-2400		2400, 60	2.15 ± 0.0	7.8 ± 2.0	6 ± 2.4	32 ± 2.0	125± 27	-
ATS-2765		2765, 30	2.08 ± 0.0	10.7 ± 1.2	~ 0	55 ± 18	92 ± 2	195
AT	4 at.%Ti	2765, 30	1.99 ± 0.2	14 ± 1.0	2.0 ± 0.7	95 ± 15	83 ± 5	218

Figure 1

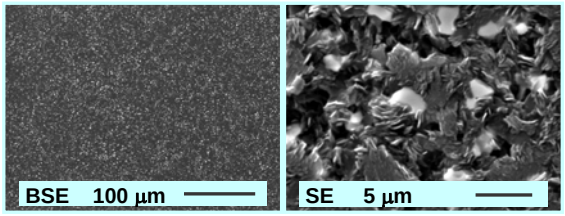

Figure 2

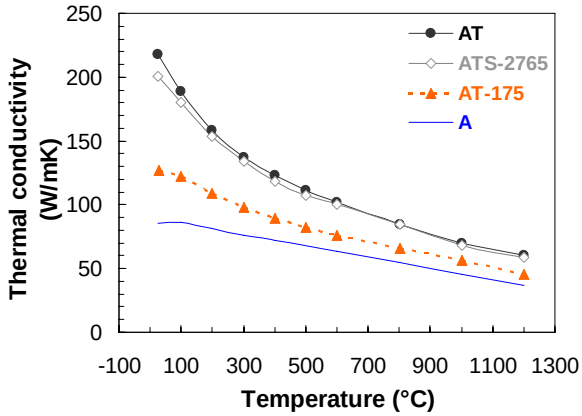
Thermal conductivity (W/mK)
250
200
150
100
50
0
-100
100
300
500
700
900
1100
1300
Temperature (°C)
AT
ATS-2765
AT-175
A

Figure 3

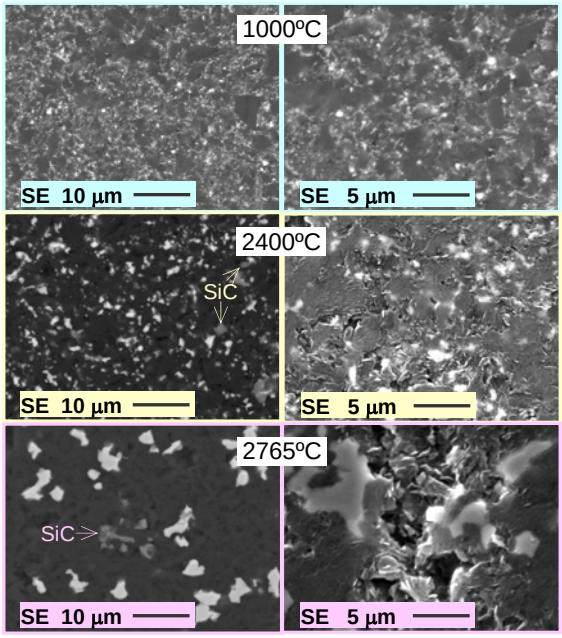
1000ºC
SE 10 µm
SE 5 µm
2400ºC
SiC
SE 10 µm
SE 5 µm
2765ºC
SiC
SE 10 µm
SE 5 µm

Figure 4